



Deciphering competing interactions of Kitaev-Heisenberg- Γ system in clusters: part II - dynamics of Majorana fermions

Sheikh Moonsun Pervez ^{1,2,*} and Saptarshi Mandal ^{1,2,†}

¹*Institute of Physics, Sachivalaya Marg, Bhubaneswar-751005, India*

²*Homi Bhabha National Institute, Training School Complex, Anushakti Nagar, Mumbai 400094, India*

(Dated: February 27, 2025)

We perform a systematic and exact study of Majorana fermion dynamics in the Kitaev-Heisenberg- Γ model in a few finite-size clusters increasing in size up to twelve sites. We employ exact Jordan-Wigner transformations to evaluate certain measures of Majorana fermion correlation functions, which effectively capture matter and gauge Majorana fermion dynamics in different parameter regimes. An external magnetic field is shown to produce a profound effect on gauge fermion dynamics. Depending on certain non-zero choices of other non-Kitaev interactions, it can stabilise it to its non-interacting Kitaev limit. For all the parameter regimes, gauge fermions are seen to have slower dynamics, which could help build approximate decoupling schemes for appropriate mean-field theory. The probability of Majorana fermions returning to their original starting site shows that the Kitaev model in small clusters can be used as a test bed for the quantum speed limit.

I. INTRODUCTION

For the last couple of decades, Kitaev model [1] has established itself as a paradigmatic model which motivated various aspects of spin-liquid physics [2–6] and many body aspect of strongly correlated condensed matter system in general. These studies can be grouped into different categories. One is the non-interacting aspect of Kitaev physics including exact fractionalization of spins [7, 8], the effect of disorder and localization [9, 10], entanglement studies [11–13] and extension to different lattices [14–17], topological degeneracies [18, 19], driven Kitaev model [8, 20], to mention a few. The second category includes a realistic effort to consider more generalized spin-Hamiltonian which includes non-Kitaev interactions such as external magnetic field [21, 22], Ising term [23], Heisenberg term [24–27] and more general interactions popularly known as J - K - Γ model [28]. Each of these studies has a common aim: to chart the exact parametric dependency where the Kitaev-spin liquid phase can be unambiguously characterized. The emergence of orbital magnetization in Kitaev magnets [29], and the possibility of tuning the exchange parameters by using light to stabilize the spin liquid phase [30], observe inverse Faraday effect [31] have been explored.

Apart from the above theoretically motivated works, contemporarily, a handful of materials have also been proposed to possess Kitaev-like interaction along with other kinds of interactions [4, 6, 24, 32–34]. The salient feature of these materials is that non-Kitaev interactions make the coveted spin-liquid state absent at very low temperatures. However, at a relatively intermediate higher temperature, the Kitaev physics - fractionalization of spins into Majorana fermions and fluxes, along with their intrinsic differences in the length and time

scale of their dynamics - enable certain aspects of Kitaev spin liquid state to be realized experimentally [35–43]. Further recent studies show that proximity effect of α - RuCl_3 in graphene heterostructure [44, 45] increases the strength of Kitaev interaction and induces an insulator to metal transition which might lead to exotic superconducting states. Such heterostructure study holds great promise for interesting application-oriented Kitaev-motivated physics to be observed in the near future.

Though a lot of work has been done to explore various aspects of the Kitaev Model, as mentioned earlier, only a limited theoretical works [27, 46, 47] attempted to investigate the dynamics of Majorana fermions (matter and gauge) for a generalized Kitaev model. In a previous study [27], matter and gauge fermion's time-dependent correlations have been investigated for J - K - Γ model using an augmented patron theory, which is limited only to few choices parameters, and effect of magnetic field has not been considered. On the other hand, though a magnetic field has been considered in [47], the study only considers a Kitaev model in the absence of Heisenberg and Γ interactions. Similarly, in the study of non-equilibrium dynamics of Majorana fermions [46], only Kitaev interaction is considered. This motivates us to explicitly investigate the dynamics of matter Majorana fermion and gauge Majorana fermions in detail within a single study for all possible parameter regions and find the effect of a magnetic field.

To this end, we have considered various small clusters, starting from four-site to twelve-site, for this purpose. The schematics of the clusters are shown in FIG.1. Though we anticipate that the Majorana dynamics may contain significant boundary effects in small clusters, studying the interplay of Majorana dynamics in small clusters is an interesting theoretical question that deserves attention. Especially the question we ask: What is the effect of competing interactions in a generalized J - K - Γ model, and how does the competition manifest in Majorana dynamics, both in matter and gauge sectors

* moonsun@iopb.res.in

† saptarshi@iopb.res.in

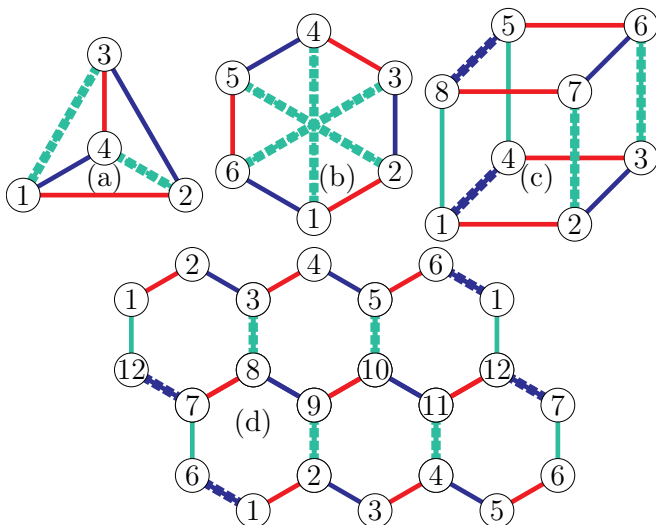


FIG. 1. Depiction of (a) 4-site, (b) 6-site, (c) 8-site, and (d) 12-site Kitaev cluster. A bond's red, blue, and green colour indicates x , y , and z -type Ising interaction between the two sites that hold that particular bond. Thickly dotted bonds are 'normal bonds', and the other bonds are 'tangent bonds', as described in the main text.

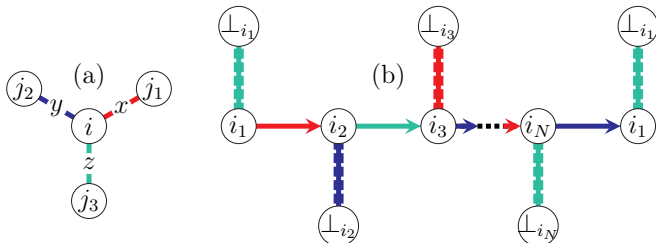


FIG. 2. (a) Basic constituent of Kitaev-type cluster; a site is connected with three neighbours with direction-dependent Ising-like interaction. (b) Typical Jordan-Wigner path for fermionization. Solid lines are tangent bonds, and dotted lines depict normal bonds.

and what is the role of external magnetic field on these. To our surprise, in our exact numerics, we have explored interesting aspects such as magnetic field can potentially make the gauge fermions conserved and behave similarly to the non-interacting limit. Further, we found that certain aspects of quantum speed limit can be studied in these systems. The presentation in this paper is organized as follows. First, we introduce the various clusters we considered, the exact Jordan-Wigner transformation used, and the order parameter considered in section II. The result of gauge and matter fermions dynamics are described in section III. We conclude with a discussion in section IV.

II. KITAEV-CLUSTER-BASICS AND JORDAN-WIGNER FERMIONIZATION

The defining Hamiltonian we investigate in our study is the J - K - Γ model [28, 48]. We work in isotropic Kitaev limit ($K_x = K_y = K_z = K$) and fix the energy scale by setting $|K| = 1$. We use natural units, i.e., Planck constant $\hbar = 1$, and Boltzmann constant $k_B = 1$. In these units (and absorbing a $1/2$ -factor (per spin) in the parameters), the Hamiltonian becomes,

$$H = H_K + H_J + H_\Gamma + H_Z. \quad (1)$$

Where H_K is the Kitaev part of the Hamiltonian. It is direction-dependent Ising interaction on each bond and is given by,

$$H_K = K \sum_{\langle j,k \rangle_x} \sigma_j^x \sigma_k^x + K \sum_{\langle j,k \rangle_y} \sigma_j^y \sigma_k^y + K \sum_{\langle j,k \rangle_z} \sigma_j^z \sigma_k^z, \quad (2)$$

where $\sigma_j = \{\sigma_j^x, \sigma_j^y, \sigma_j^z\}$ are the spin $1/2$ Pauli operators at j^{th} site. The second term in Hamiltonian is the Heisenberg exchange interaction,

$$H_J = J \sum_{\langle j,k \rangle} \sigma_j \cdot \sigma_k, \quad (3)$$

and it is parameterized by the exchange coupling parameter J . The third term is an off-diagonal interaction, widely known as the Γ term given by,

$$H_\Gamma = \Gamma \sum_{\langle j,k \rangle_{\alpha \neq \gamma \neq \delta}} \sigma_j^\alpha \sigma_k^\delta + \sigma_k^\gamma \sigma_j^\delta. \quad (4)$$

The last term in Hamiltonian denotes the effect of the external Zeeman field taken along z -direction. It is well known that a pure Kitaev model is described by a non-interacting Majorana fermion hopping problem ($H = \sum_{jk} J_{jk} i c_j c_k$), in the background of conserved Z_2 gauge fields $u_{ij} = i b_i b_j$ [1]. In the appropriate representation, these conserved gauge field operators can be re-written as an equivalent number operator as $u_{ij} = 2\chi^\dagger \chi - I$, named bond-fermions [7, 19]. The Majorana operator (c_i) can also be appropriately recast in terms of complex fermion ψ , which on some bonds appear as $2\psi^\dagger \psi - I$. The non-Kitaev interactions in the Hamiltonian given in Eq.1 make the gauge fields acquire dynamics as they are no longer conserved. Quantitative analysis of these matter and gauge fields' dynamics are essential ingredients to understand the possible spin-fractionalization leading to spin-liquid phase appearing at intermediate temperature [40, 49–51]. This is also intimately connected to confinement-deconfinement transitions associated with the magnetically ordered state to quantum paramagnetic states, including the Kitaev spin liquid state.

The original solution of Kitaev [1] suffers from enlargement of Hilbert space, and to avoid that, here we implement Jordan-Wigner transformation (JWT), as

outlined in a previous study [52]. Below, we briefly describe the salient features of the implementation of JWT.

Fermionization procedure (‘fermionic decoupling’): The one-dimensional path for JWT is taken along $1 \rightarrow 2 \rightarrow 3 \rightarrow \dots \rightarrow N-1 \rightarrow N \rightarrow 1$ (FIG. 2), and bonds on this path are called tangent bonds; the bonds which are not on this path, are normal bonds (dotted bonds in FIG. 1 and FIG. 2). To do JWT, we define the Jordan-Wigner string operator μ_{i_m} as,

$$\mu_{i_m} = \prod_{j=1}^{m-1} \hat{n}_{i_j} \cdot \sigma_{i_j}, \quad (5)$$

where, \hat{n}_{i_j} is the normal direction from the j^{th} site, denoted as i_j . JW Fermions at site i_m are ,

$$\begin{aligned} \eta_{i_m} &= (\hat{t}_{1,i_m} \cdot \sigma_{i_m}) \mu_{i_m}, \\ \xi_{i_m} &= (\hat{t}_{2,i_m} \cdot \sigma_{i_m}) \mu_{i_m}, \end{aligned} \quad (6)$$

where, $\hat{t}_{1(2),i_m}$ is the in(out)-going tangent direction at site i_m while walking along the JW path. Note that η_{i_m} and ξ_{i_m} are essentially Majorana fermions and note that, alternatively, one can express σ 's in terms of η, ξ as shown below,

$$\begin{aligned} \hat{t}_{1,i_m} \cdot \sigma_{i_m} &= \eta_{i_m} \mu_{i_m}; & \hat{t}_{2,i_m} \cdot \sigma_{i_m} &= \xi_{i_m} \mu_{i_m}; \\ i \eta_{i_m} \xi_{i_m} &= i (\hat{t}_{1,i_m} \cdot \sigma_{i_m}) (\hat{t}_{2,i_m} \cdot \sigma_{i_m}) = \hat{n}_{i_m} \cdot \sigma_{i_m}. \end{aligned} \quad (7)$$

With these definitions, spin-spin interaction in Hamiltonian is written in terms of η, ξ , and the trailing operator μ . The trail operator for the end bond ($N \rightarrow 1$) is $S = \prod_{j=1}^N \sigma_{i_j}^{\perp}$. We combine the Majorana operators to define the complex fermions on normal bonds as $\eta_{i_k} = \psi_{i_k} + \psi_{i_k}^\dagger$; $\eta_{\perp i_k} = \frac{1}{i}(\psi_{i_k} - \psi_{i_k}^\dagger)$ and $\xi_{i_k} = \chi_{i_k} + \chi_{i_k}^\dagger$; $\xi_{\perp i_k} = \frac{1}{i}(\chi_{i_k} - \chi_{i_k}^\dagger)$. With these definitions of η 's and ξ 's, the terms in Hamiltonian are written in terms of χ and ψ and in general it is an interacting Hamiltonian. We follow exact diagonalization in suitable occupation number representations of χ and ψ fermions and obtain the exact eigenstates to analyze the Majorana dynamics.

Dynamics of Majorana fermions: To investigate the fermion dynamics, we define the density-density correlation as,

$$g(t) = \langle \text{GS} | e^{iHt} \hat{N}_i e^{-iHt} \hat{N}_i | \text{GS} \rangle, \quad (8)$$

where $|\text{GS}\rangle$ is the ground state of the system, and the number operator \hat{N}_i is defined as,

$$\begin{aligned} \hat{N}_i &= 2 \chi_i^\dagger \chi_i - I \quad \text{for Gauge fermions,} \\ &= 2 \psi_i^\dagger \psi_i - I \quad \text{for Matter fermions,} \end{aligned} \quad (9)$$

for $i = [1, \frac{N}{2}]$. We note that $g(t)$, in general, is a complex number, and we plot its absolute value. This can be

simplified further considering $\hat{N}_i |\text{GS}\rangle = \sum_n c_n |n\rangle$ where $|n\rangle$ denotes the n^{th} eigenstate, yielding $g(t) = \sum_n |c_n|^2 e^{-i(E_n - E_0)t}$. Here E_n is the energy corresponding to $|n\rangle$ and E_0 is the ground state energy, and $c_n = \langle n | \hat{N}_i | \text{GS} \rangle$. Physically, $g(t)$ measures how the *fermionic density* changes over time under unitary evolution at a given site, with respect to its initial value $g(0)$. The initial value has been effectively normalized to 1.

We have chosen \hat{N}_i of the above form because they have a similar form of the conserved operator u_{ij} associated with a given bond. However we notice that, $\langle \hat{N}_i^{(\psi)}(t) \hat{N}_i^{(\psi)}(0) \rangle = \langle (2\psi_i^\dagger \psi_i(t) - I)(2\psi_i^\dagger \psi_i(0) - I) \rangle = \langle 4n_i^{(\psi)}(t)n_i^{(\psi)}(0) - 2n_i^{(\psi)}(t) - 2n_i^{(\psi)}(0) + I \rangle$. Where we have used $n_i^{(\psi)} = \psi_i^\dagger \psi_i$. We note that $\langle n_i^{(\psi)}(t) \rangle = \langle n_i^{(\psi)}(0) \rangle$. Thus, effectively, $g(t)$ depends on $\langle n_i(t)n_i(0) \rangle$. We note that $n_i^{(\psi)}(n_i^{(\chi)})$ acts as a projector on the ground state such that it only projects states with ψ (χ) fermion on the i^{th} bond. Thus, $g(t)$ yields the probability amplitude of those states to return to itself. In pure Kitaev limit, as $\hat{N}_i^{(\chi)}$ is static, $g_\chi(t)$ is constant in time but acquires time dependence once non-Kitaev terms are included. In the presence of these other interactions, ψ and χ interact; thus, estimating those quantities in Eq. 8 yields an understanding of the dynamics associated with non-Kitaev interactions. The next section summarises the salient characteristics of the gauge and matter Majorana fermion dynamics.

III. DYNAMICS OF GAUGE AND MATTER SECTOR

To describe the dynamics of Majorana fermions, we consider bonds (1,3), (1,4), (1,4), (1,6) for 4, 6, 8, and 12-site cluster (‘normal bonds’ [19] connected with the first site). Thus, in the text below, whenever we mention χ or ψ fermion, it is to be understood that they are defined on these bonds. Occasionally, for the 8-site and 12-site clusters, we mention χ_2 , which are defined on bonds (2,7) and (2,9), respectively; these are fermions on a z -type normal bond (unlike the y -type normal bonds that are connected with the first site in these two clusters). This helps us to compare the results from the four and six-site clusters, which hold z -type normal bonds connected with the first site. Moreover, we describe the amplitude of $|g(t)|$ with respect to its value in the pure-Kitaev limit. That is, ‘zero amplitude’ means $|g(t)| = 1$, and ‘large amplitude’ (away from $|g(t)| = 1$, and closer to $|g(t)| = 0$) means it has deviated from the Kitaev limit.

Qualitative differences between four-site cluster and other clusters: In all of the parameter regimes, there are qualitative differences in the dynamics of gauge fermions between the four-site cluster and other larger clusters. For $\Gamma = 0 = J$, the dynamics of gauge fermions

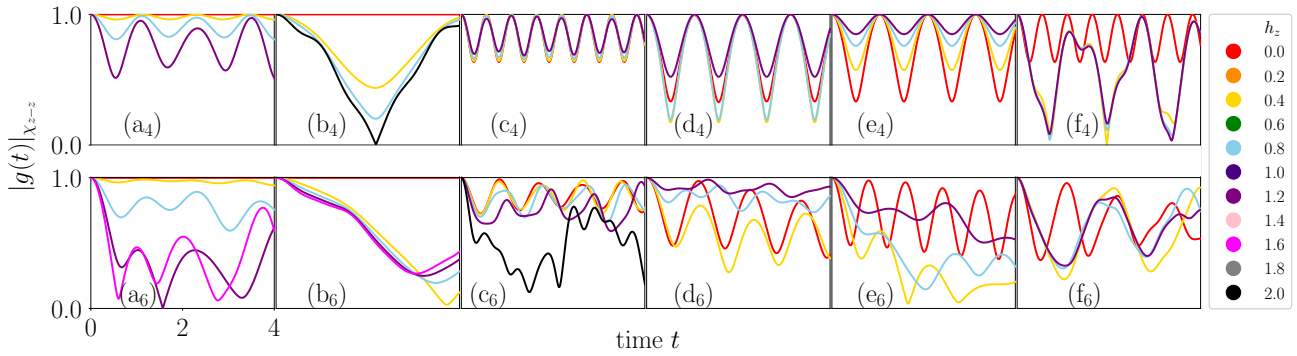


FIG. 3. Gauge Majorana dynamics for $\Gamma = 0$ and (a_N) $K = 1.0$, $J = 0.0$, (b_N) $K = -1.0$, $J = 0.0$, (c_N) $K = 1.0$, $J = 0.5$, (d_N) $K = -1.0$, $J = 0.5$, (e_N) $K = 1.0$, $J = -0.5$, (f_N) $K = -1.0$, $J = -0.5$. Different strengths of h_z are given in the legend box.

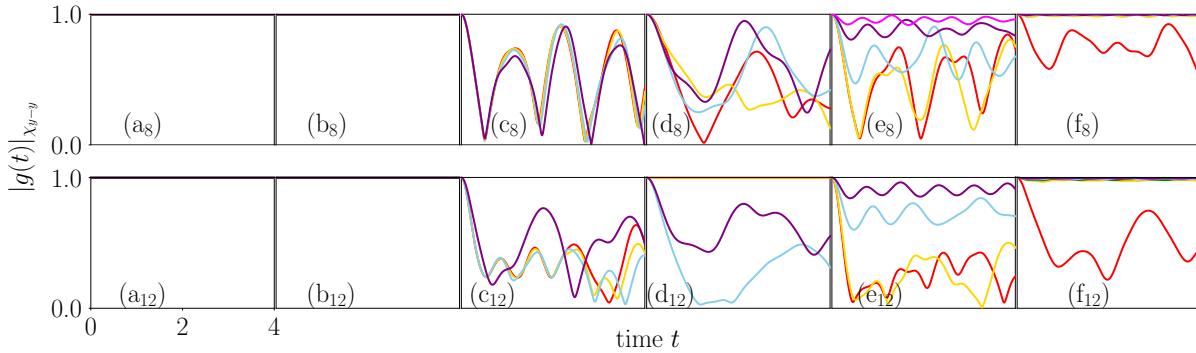


FIG. 4. Gauge Majorana dynamics for $\Gamma = 0$ and (a_N) $K = 1.0$, $J = 0.0$, (b_N) $K = -1.0$, $J = 0.0$, (c_N) $K = 1.0$, $J = 0.5$, (d_N) $K = -1.0$, $J = 0.5$, (e_N) $K = 1.0$, $J = -0.5$, (f_N) $K = -1.0$, $J = -0.5$. Different strengths of h_z are given in the legend box of FIG.3.

are very regular and periodic as we vary the external magnetic field. For intermediate AFM J , the oscillations are very regular. Amplitude decreases monotonously as we increase the strength of h_z (see FIG.3, panel (e₄)). However, for FM J , appearances of additional frequency could be noticed (FIG.3, panel (f₄), which points out that the ground state is modified differently than the AFM case. In the 4-site cluster, when we do the ground state analysis, for $K = 1$, $J = -0.5$, gauge dynamics can be calculated analytically to get $|g(t)| = \frac{1}{3}(5 + 4\cos(12Jt))^{1/2}$ at $h_z = 0$. When h_z is introduced, only diagonal elements of the Hamiltonian are modified, leading to an equally tractable analytic calculation to see that $|g(t)| = \left| |\alpha|^2 + |\tilde{\alpha}|^2 + 4|\beta|^2 e^{-12iJt} \right|$, where the ground state is represented in the form $\alpha|\uparrow_1\uparrow_2\uparrow_3\uparrow_4\rangle + \tilde{\alpha}|\downarrow_1\downarrow_2\downarrow_3\downarrow_4\rangle + \beta(|\uparrow_1\downarrow_3\rangle - |\downarrow_1\uparrow_3\rangle)(|\uparrow_2\downarrow_4\rangle - |\downarrow_2\uparrow_4\rangle)$. The same expression for $g(t)$ is true for any $J = -K/2$ in the 4-site cluster in the absence of Γ .

The same qualitative difference discussed above can also be seen for matter fermions. However, we notice that, in general, the average amplitude of oscillations for gauge fermions is always larger than the matter fermions. This can be attributed to the non-local nature of the gauge fermions in terms of the spin operators and

the fact that each flux sector is separated by an energy gap much larger than the fermionic spectrum for each flux sector.

Regular oscillations and irregular oscillations: It is observed that depending on the h_z , gauge fermion oscillation could be regular to irregular type. For example, consider the 6-site cluster at $J = 0$. Up to $h_z = 0.6$, the oscillations are minimal, but after that, it suddenly increases[53] and reaches a maximum for $h_z = 1.2$ and decreases again. This has been shown in FIG.3, panel (a₆). On numerous occasions, it has been observed that h_z can reverse the response of gauge fermions amplitude or time period of oscillations. For the 8-site cluster, a different scenario is observed, comparing $J = -0.5, 0.0, 0.5$. In FIG.4, panel (e₈, f₈), for $J = -0.5$, the amplitude of oscillation decreases with the increase of h_z . For $J = 0.5$ (FIG.4, panel (c₈, d₈)), the oscillations remain more or less the same for all h_z ; no special feature is seen. However, for the 12-site cluster, such a non-monotonous response is absent. Very interestingly, we see from FIG.4 panel (a₈, b₈, a₁₂, b₁₂) that the gauge fermion does not show any dependency on time for any h_z . This can be referred to as stabilizing gauge fields under an external magnetic

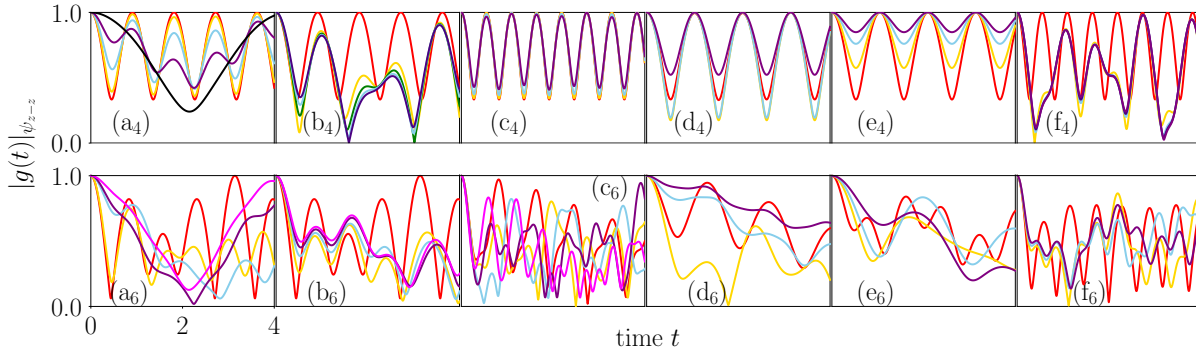


FIG. 5. Matter Majorana dynamics for $\Gamma = 0$ and (a_N) $K = 1.0$, $J = 0.0$, (b_N) $K = -1.0$, $J = 0.0$, (c_N) $K = 1.0$, $J = 0.5$, (d_N) $K = -1.0$, $J = 0.5$, (e_N) $K = 1.0$, $J = -0.5$, (f_N) $K = -1.0$, $J = -0.5$. Different strengths of h_z are given in the legend box of FIG.3.

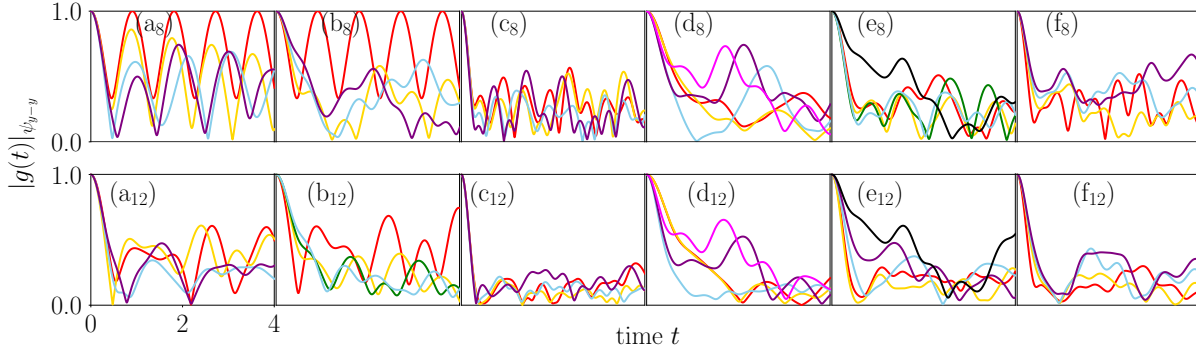


FIG. 6. Matter Majorana dynamics for $\Gamma = 0$ and (a_N) $K = 1.0$, $J = 0.0$, (b_N) $K = -1.0$, $J = 0.0$, (c_N) $K = 1.0$, $J = 0.5$, (d_N) $K = -1.0$, $J = 0.5$, (e_N) $K = 1.0$, $J = -0.5$, (f_N) $K = -1.0$, $J = -0.5$. Different strengths of h_z are given in the legend box of FIG.3.

field on certain bonds. This happens for gauge fermions defined on a y -type bond and when the magnetic field is applied along \hat{z} -direction. However, on a different bond, the gauge fermion dynamics is oscillatory, as shown in FIG.7. There, we have shown dynamics of χ_2 gauge fermion, which is defined on a z -type bond, and it does show dynamics under the influence of magnetic field applied along the \hat{z} -direction. The above-controlled manipulation of gauge field dynamics could be of practical use.

The identical trends can also be seen for matter fermions, depending on the relative strength of h_z and J . For example, one can compare $(N, K, J, h_z) = (6, 1, 0, 0.4)$ and $(6, 1, 0, 1.2)$. In the former case, many minimums are found, but for the latter, only a single minimum was found; see FIG.5, panel (a₆). The nature of oscillation completely changed. Similar trends are there for $(N, K, J, h_z) = (6, -1, 0.5, 0)$, $(6, -1, 0.5, 0.4)$, $(6, -1, 0.5, 0.8)$, i.e., panel (d₆) in FIG.5 (for ψ_2 fermion (matter fermion defined on a different bond) too, we see equivalent trends). These three sets of parameters yield three different behaviours for the matter fermion. For 8-site cluster, such differences are also found for $(K, J) = (-1, -0.5)$, $(-1, 0)$, $(-1, 0.5)$ (see FIG.6, panel

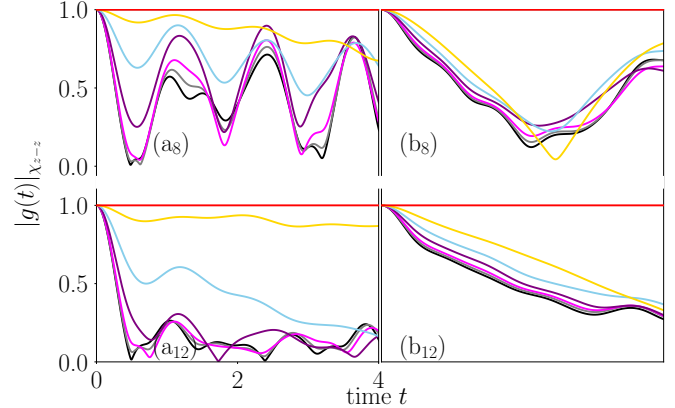


FIG. 7. Evolution of gauge fermion defined on a z -type bond in (a₈, b₈) 8-site, and in (a₁₂, b₁₂) 12-site cluster. Parameter values are, $J = 0$, $\Gamma = 0$, along with (a_N) $K = 1$ and (b_N) $K = -1$. Colour coding for different magnetic fields is the same as given in the legend box of FIG.3.

(b₈, d₈, f₈)), and also for $(K, J) = (1, 0)$, $(1, 0.5)$, $(1, -0.5)$ (panel (a₈, c₈, e₈)), where depending on external magnetic field, matter fermion's dynamics changes a lot. Similarly, for 12-site, the relevant set of parameters for such change

in the nature of dynamics for matter fermion can be seen at $(K, J)=(1, -0.5), (-1, 0.5)$.

Dependency of average amplitude and time period of oscillations on h_z and J : Interestingly, it has been noticed that for $J = 0$, the time period of oscillations is much larger for $K = -1$ than $K = 1$ case; this can be noticed from the first and second columns of FIG.5 and FIG.6. In the first column, for finite h_z , the oscillations have more amplitude and time period than the second column. However, as we turn on finite J , the time period of oscillations becomes comparable, though it greatly depends on the relative strength of K , J and h_z . It is also observed that the external magnetic field helps revive the amplitude of matter fermion on that site. For example, consider the 12-site cluster where the rapid fluctuations are absent compared to smaller clusters. If we look at $(K, J) = (-1, 0.5)$ (FIG.6, panel (d₁₂)), where in between $t = 1$ and $t = 3$, there is a revival of amplitude of matter fermions. Similarly we find for $(K, J) = (1, 0)$ (panel (a₁₂) with $h_z = 0.4$) $(K, J) = (\pm 1, -0.5)$ (panel (e₁₂, f₁₂)). Similarly we see that for gauge fermions, $(K, J) = (-1, 0)$ corresponds to larger time period in comparison to $(K, J) = (+1, 0)$.

Two different channels of dynamics of oscillations: It is also noted that depending on the initial position of the matter fermions, its time dependency could be very different. For comparison, we note the results for the 12-site cluster with the parameter value $(K, J, \Gamma) = (-1, 0.5, 0)$, as shown in FIG.8.

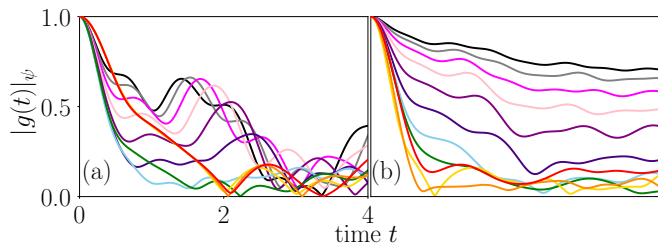


FIG. 8. Evolution of matter sector which is defined on (a) bond (1-6: a y -type bond) and (b) bond (2-9: a z -type bond), for $K = -1$, $J = 0.5$, and $\Gamma = 0$, in the 12-site cluster. Different strengths of h_z are the same as shown in the legend box of FIG.3.

We observe that whereas ψ_1 (defined on a y -type bond) decays rapidly, ψ_2 (defined on a z -type bond) has quite small oscillations and varies smoothly. The average magnitude of $g_\psi(t)$ corresponding to ψ_2 also gradually decreases consistently with increasing h_z . Depending on the initial position of the matter fermion, this different behaviour indicates local competition between different interactions, such as Heisenberg and Kitaev interaction. The same applies to FM J with parameter $(K, J) = (-1, -0.5)$. There is a marked difference in the dynamics of ψ_1 and ψ_2 . The same can be said for $J = 0$.

This observation could be beneficial for the controlled manipulation of Majorana fermions for useful quantum state operations.

Stabilization of Z_2 gauge field by external magnetic field: It has been observed that, as the applied magnetic field is in z -direction, it can stabilize the Z_2 (defined on a z -type bond) gauge field[54] as seen in for eight and twelve-site cluster $(K, J)=(-1, -0.5)$ (FIG.4, panel (f₈, f₁₂)). For intermediate value of positive J , the gauge field fluctuation decreases as we increase h_z as seen for $(K, J)=(-1, 0.5)$ (FIG.3, panel(d₆)). This can be thought of as stabilizing the spin-liquid or fractionalized state by an external magnetic field. For AFM J , the Z_2 gauge fields show more oscillatory patterns than FM J , where they become closer to unity.

Gauge fermion dynamics in the plateau region of correlation: In our previous study [55], we have shown that in these clusters, in the presence of AFM J , the correlation function can show a plateau region where the ground state effectively does not change over a range of J or h_z . So, it will be interesting to investigate the fate of gauge field dynamics in this plateau region.

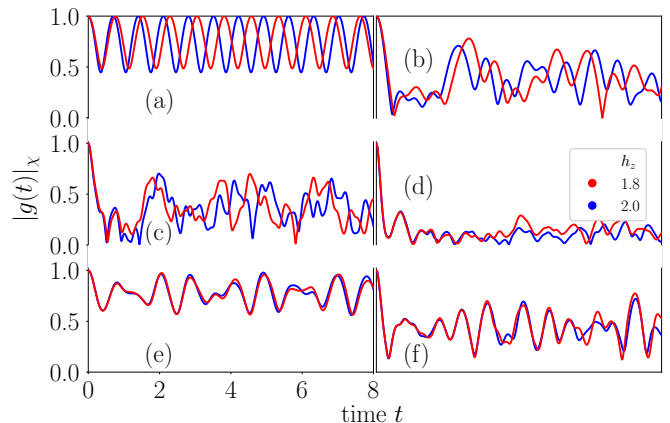


FIG. 9. Evolution of gauge sector in the plateau region of correlation. (a) 4-site result; χ is defined on bond (1-3: a z -type bond), and $K = 1$, $J = 0.40$, $\Gamma = 0$. (b) 6-site result; χ is defined on bond (1-4: a z -type bond), and $K = 1$, $J = 0.13$, $\Gamma = 0$. In 8-site, for $K = 1$, $J = 0.70$, $\Gamma = 0$ (c) χ is defined on bond (2-7: a z -type bond), and (e) χ is defined on bond (1-4: a y -type bond). In 12-site, for $K = 1$, $J = 1.00$, $\Gamma = 0$ (d) χ is defined on bond (2-9: a z -type bond), and (f) χ is defined on bond (1-6: a y -type bond). Different strength of h_z is as shown in the legend box.

In FIG.9, we study $|g(t)|_\chi$ in the clusters for specific J values as mentioned in the caption. At these J values, for $h_z = 1.8$ and 2.0 , correlation does not change for the respective cluster. As we observe, dynamics for $h_z = 1.8$ is commensurate with that for $h_z = 2.0$. Surprisingly, for χ fermion defined on a y -type bond (panel (e,f) of FIG.9), the dynamics are almost identical for these two different strengths of h_z . This shows how the gauge

fermions' dynamics really depend on the magnetic field's direction.

Scenarios to define quantum speed limit (QSL) : Recently, various aspects of the QSL, as defined by the evolution of a quantum state from a given state to a distinctly different state, attracted wide interest for various reasons [56–59]. In this context, we find that QSL could be investigated for the evolution of Majorana fermions. Initially, they begin with a given occupancy at a given bond. If the fermion occupation on that bond becomes zero at any future time, we can define QSL for our system. In this study of dynamics for gauge and matter fermions, we witness numerous occasions where such a situation occurs.

The fascinating occurrence of QSL happens for 4-site cluster with $(N, K, J, h_z) = (4, -1, 0, 2)$, $(4, -1, -0.5, 0.4)$ (panel (b₄, f₄) of FIG.3 and FIG.5). This happens in both the matter and gauge fermion sector. For the second set of parameters, they are remarkably repetitive with time. For AFM K , such realization does not happen (in the 4-site cluster) except for very large FM J . In 6-site cluster for the gauge fermions, we find $(N, K, J, h_z) = (6, 1, 0, 1.2)$ being such an example (panel (a₆), FIG.3). For large AFM J , it also happens for matter fermions. There are occasions for gauge fermions on other bonds too for such phenomena, for example at $(N, K, J, h_z) = (8, -1, 0, 0.4)$ in χ_2 gauge fermion (FIG.7, panel (b₈)), and $(N, K, J, h_z) = (8, 1, 0, 1.8)$, $(8, 1, 0, 2.0)$ (FIG.7, panel (a₈)). There are special cases where such phenomena are also observed for the 12-site cluster. A careful study and estimation of this QSL will be done in future studies as this is not the primary focus here.

The main differences in the dynamics of Majorana fermions between twelve-site cluster and other clusters : The most apparent difference between 12-site and other smaller clusters can be understood by analyzing $J = 0$. In the absence of J , gauge fermion remains constant with time for clusters of all sizes when the external field is not there. However, matter fermions oscillate with fixed frequency and return to unity after characteristic time for four and eight-site clusters due to the backflow from the boundary. On the other hand, for the 6-site cluster, the matter fermions return to unity after a few local maxima. However, for the 12-site cluster, the matter fermions *never* return to unity (the time for returning is $t \sim 5 \times 10^2$, which is two orders of magnitude larger than the other three smaller clusters). Secondly, for finite J , the oscillations in χ or ψ fermions have a regular pattern for different h_z , but for smaller clusters, the pattern of dynamics varies greatly depending on h_z .

The appearance of multiple frequencies in the dynamics of Majorana fermions can be understood as follows. For a fixed gauge field configuration, the effective Hamiltonian for ψ fermions reduces to a superconducting

Hamiltonian with the presence of $\eta_{ij}\psi_i\psi_j + h.c.$ The ground state |GS) is constructed as the vacuum of the quasi-particles where the states with an even number (including zero) of ψ fermions appear with different probability amplitude. Now the operator $n_i^{(\psi)} = \psi_i^\dagger\psi_i$ selects (or projects) only those states with the dimer 'i' being occupied. These daughter states could be re-expressed as linear combinations of all the eigenstates (including excited and ground states) with different amplitudes. Thus the final expression of $g_\psi(t)$ contains the summation of $\sum_n A_n \exp^{-i(E_n - E_0)t}$ where the detail analytic expression of A_n is in general very complex. With a system size very large, substantial contribution to A_n coming from numerous daughter states makes the probability amplitude oscillate with no fixed time period.

Now, for finite non-Kitaev interaction being present, the gauge fermions are no longer conserved, and hence, they also oscillate with time. Due to special symmetry, the matter and gauge fermion return to unity with identical frequency for the 4-site cluster. As the cluster size increases, the oscillations of matter and gauge fermions become irregular due to contributions from the increasing number of excited states for larger clusters. However, few universal characteristic features are present. One notes that, on average, the gauge fermion amplitude is always larger than the matter fermion. Also, matter fermions complete many cycles of oscillations within a given time window compared to gauge fermions. This points out that gauge fermions can still be approximated as slow varying background conserved operators for the matter fermions and hence may support the survival of the deconfined phase.

Dynamics of matter and gauge fermions at $\Gamma \neq 0$

Next, we focus on the case where finite Γ is present. For the sake of simplicity, we only describe the analysis in the absence of J . Corresponding plots are given in FIG.10,11,12,13, in Appendix A.

Gauge fermion dynamics at $\Gamma = \pm 0.5$: When we compare the results of AFM K (first and third column of FIG.10 and FIG.11) with that of FM one (second and fourth column), we observe that gauge fermions fluctuate more in FM K case. However, crucial differences exist among the clusters. In 4 and 6-site, with increasing magnetic field, $|g(t)|$ gradually moves away from its initial value of 1, whereas, in 8 and 12-site clusters, it moves closer to 1. Also, when we notice that in the 4-site cluster, for FM K , $g(t)$ at high magnetic fields contain lower frequency and with lesser h_z , overall frequency is a little high (panel (b₄, d₄), FIG.10). In the 6-site cluster, depending on the sign of Γ and K , different h_z mainly yield two different behaviours. For lower magnetic fields, $g(t)$ remains closer to its initial value, and at relatively higher h_z , $g(t)$ moves closer to zero. In larger clusters (8

and 12 sites), this kind of different behaviour, depending on h_z , is absent. We observe $g(t)$ vanishes immediately as we introduce Γ (red line in FIG.11), which gets revived as we gradually increase h_z .

Matter fermion dynamics at $\Gamma = \pm 0.5$: Here, we refer to FIG.12 and FIG.13 of Appendix A. Firstly, as we increase the system size, $g(t)$ gradually vanishes, even without a magnetic field. However, for a smaller cluster, there is a higher chance for the fermion to return to its initial state due to reflection. In addition, at lower h_z , fluctuation in $g(t)$ is more prominent for four and six-site than higher values of h_z . However, for larger clusters, an increase in h_z only makes $g(t)$ away from zero. In the 12-site cluster (panel (a₁₂,b₁₂,c₁₂,d₁₂) of FIG.13), the fermion never returns to its initial state. This happens because as the system evolves with time, the fermion gradually diffuses into the bulk, and the reflection from the boundary is ineffective in returning to its initial position because of the cluster's large size.

IV. DISCUSSION

As mentioned earlier, the Kitaev model contains two types of Majorana fermions: matter Majorana fermions and gauge Majorana fermions. In the Kitaev limit, two gauge Majorana fermions combine to constitute a conserved Z_2 flux operator. On the other hand, matter Majorana fermions constitute a non-interacting hopping problem coupled to this conserved Z_2 field. However, with other non-Kitaev interactions, gauge fermions acquire dynamics. Various interesting consequences arise, such as the confinement-deconfinement transition, related to the revival of the spin-liquid phase at intermediate temperatures. The time evolution of matter and gauge fermions follow an oscillatory yet decaying pattern depending on different interactions. These oscillations have various interesting profiles, but their dependency on the external magnetic field is the most significant. The external magnetic field is seen to modulate significantly the amplitude of oscillations and also the average magnitude of it. Depending on the strength of the external magnetic field, it can freeze the gauge field without having any oscillations, showing remarkable dependence on the magnetic field.

In pure Kitaev limit, the gauge fields are static; effectively, they are *infinitely heavy*. With the application of magnetic field, they become *lighter*. A higher magnetic field makes the gauge fermion diffuse more into the bulk, as can be seen via a higher amplitude of $|g(t)|$. The frequency of oscillation in FM K is smaller than AFM K . Next, we introduce non-zero Heisenberg strength and find that the dynamics are qualitatively similar for a competing J and K . In both cases ($\pm K$ and $\mp J$), an increase in magnetic field results in a $|g(t)|$, which remains close to its initial value. When

the sign of J and K are the same, the overall picture tells us that the increasing h_z makes the amplitude of $|g(t)|$ reach closer to zero, indicating the fermionic density to be more diluted. Next, we looked at finite Γ results in the absence of J . The gauge field dynamics are controlled mainly by K , with minimal effect from AFM or FM Γ . In the presence of Γ , increasing h_z makes $|g(t)|$ to have higher amplitude for AFM K , whereas for FM K , a gradual increase in h_z results in a $|g(t)|$ which approaches its initial value. In all cases, a bigger cluster shows slower dynamics, owing to the larger size, for it has more room for the fermion to get diluted. For some parameter values, the gauge field dynamics are seen to be stabilized by applying a magnetic field of proper magnitude and direction.

Next, we study the dynamics of matter fermions. A higher magnetic field on top of the Kitaev interaction case makes the matter fermion diffuse more. The frequency of oscillation in FM K is smaller. Then we put non-zero Heisenberg strength and find out that, for a competing J and K , just like the gauge dynamics, the matter dynamics are qualitatively similar here, too. In both cases, an increase in h_z results in a $|g(t)|$ which approaches 1. Next, we study finite Γ results in the absence of J . We find that the matter field dynamics are influenced mainly by K , with little respect towards AFM or FM Γ . In the presence of Γ , increasing h_z makes the matter fermion dilute less into the bulk for FM K . In every case, a larger cluster shows slower dynamics.

On a different note, the 6-site cluster that we have considered here has a resemblance with the hexagonal-plaquette taken previously [60] (which contains next to next nearest neighbour interaction) after swapping a pair of sites (site-3 and site-5, to be specific) or by site-dependent gauge transformations. Thus, it is related to a physically motivated extended Kitaev model.

In the plateau region of correlation, where the ground state *almost* remains the same for a range of magnetic field (in \hat{z} -direction) values, for a given Heisenberg and Kitaev interaction, the gauge dynamics is *almost* identical when we look at the dynamics of a gauge field defined on a y -type bond. Meanwhile, gauge fermion, defined on a z -type bond, shows commensurate dynamics for multiple magnetic fields. An interesting realization of quantum speed limit(QSL) phenomena also appears where the probability of Majorana fermion vanishes from the initial value of unity. A detailed analysis of this QSL and its dependency on Heisenberg coupling and the external magnetic field will be followed in future studies.

With the recent intense effort to understand the Kitaev-Heisenberg- Γ system, we think our extensive analysis would serve as a helpful reference. However, all the aspects found here may not be readily general-

ized to the thermodynamic system. Instead, it would be prudent to consider this an exciting platform to quantify the quantum and thermal fluctuations in the Kitaev-Heisenberg- Γ system and use it to understand the thermodynamic system better. Further it may be interesting to examine Kitaev-Heisenberg model on other trivalent lattices[16, 61, 62] to find quantitative differences in comparison to Honeycomb lattice which we leave for future study.

ACKNOWLEDGEMENT

S.M.P. acknowledges SAMKHYA (High-Performance Computing facility provided by the Institute of Physics, Bhubaneswar) for the numerical computation. S.M.P. also thanks Arnob Kumar Ghosh for useful discussions. S.M. acknowledges support from ICTP through the Associate's Programme (2020-2025). S.M. also thanks G. Baskaran and Nicola Seriani for the interesting discussions.

-
- [1] A. Kitaev, "Anyons in an exactly solved model and beyond," *Annals of Physics* **321**, 2–111 (2006), january Special Issue.
- [2] L. Savary and L. Balents, "Quantum spin liquids: a review," *Reports on Progress in Physics* **80**, 016502 (2016).
- [3] L. Balents, "Spin liquids in frustrated magnets," *Nature* **464**, 199–208 (2010).
- [4] M. Hermanns, I. Kimchi, and J. Knolle, "Physics of the kitaev model: Fractionalization, dynamic correlations, and material connections," *Annual Review of Condensed Matter Physics* **9**, 17–33 (2018), <https://doi.org/10.1146/annurev-conmatphys-033117-053934>.
- [5] A. Loidl, P. Lunkenheimer, and V. Tsurkan, "On the proximate kitaev quantum-spin liquid α -rucl₃: thermodynamics, excitations and continua," *Journal of Physics: Condensed Matter* **33**, 443004 (2021).
- [6] S. Trebst and C. Hickey, "Kitaev materials," *Physics Reports* **950**, 1–37 (2022), kitaev materials.
- [7] G. Baskaran, S. Mandal, and R. Shankar, "Exact results for spin dynamics and fractionalization in the kitaev model," *Phys. Rev. Lett.* **98**, 247201 (2007).
- [8] S. Sarkar, D. Rana, and S. Mandal, "Defect production and quench dynamics in the three-dimensional kitaev model," *Phys. Rev. B* **102**, 134309 (2020).
- [9] W.-H. Kao and N. B. Perkins, "Disorder upon disorder: Localization effects in the kitaev spin liquid," *Annals of Physics* **435**, 168506 (2021), special issue on Philip W. Anderson.
- [10] J. Nasu and Y. Motome, "Thermodynamic and transport properties in disordered kitaev models," *Phys. Rev. B* **102**, 054437 (2020).
- [11] H. Yao and X.-L. Qi, "Entanglement entropy and entanglement spectrum of the kitaev model," *Phys. Rev. Lett.* **105**, 080501 (2010).
- [12] S. Mandal, M. Maiti, and V. K. Varma, "Entanglement and majorana edge states in the kitaev model," *Phys. Rev. B* **94**, 045421 (2016).
- [13] N. C. Randeep and N. Surendran, "Topological entanglement entropy of the three-dimensional kitaev model," *Phys. Rev. B* **98**, 125136 (2018).
- [14] H. Yao and S. A. Kivelson, "Exact chiral spin liquid with non-abelian anyons," *Phys. Rev. Lett.* **99**, 247203 (2007).
- [15] G. Kells, D. Mehta, J. K. Slingerland, and J. Vala, "Exact results for the star lattice chiral spin liquid," *Phys. Rev. B* **81**, 104429 (2010).
- [16] S. Mandal and N. Surendran, "Exactly solvable kitaev model in three dimensions," *Phys. Rev. B* **79**, 024426 (2009).
- [17] T. Eschmann, P. A. Mishchenko, K. O'Brien, T. A. Bojesen, Y. Kato, M. Hermanns, Y. Motome, and S. Trebst, "Thermodynamic classification of three-dimensional kitaev spin liquids," *Phys. Rev. B* **102**, 075125 (2020).
- [18] S. Mandal and N. Surendran, "Fermions and nontrivial loop-braiding in a three-dimensional toric code," *Phys. Rev. B* **90**, 104424 (2014).
- [19] S. Mandal, R. Shankar, and G. Baskaran, "Rvb gauge theory and the topological degeneracy in the honeycomb kitaev model," *Journal of Physics A: Mathematical and Theoretical* **45**, 335304 (2012).
- [20] S. Sasidharan and N. Surendran, "Periodically driven three-dimensional kitaev model," *Physica Scripta* **99**, 045930 (2024).
- [21] K. S. Tikhonov, M. V. Feigel'man, and A. Y. Kitaev, "Power-law spin correlations in a perturbed spin model on a honeycomb lattice," *Phys. Rev. Lett.* **106**, 067203 (2011).
- [22] A. Lunkin, K. Tikhonov, and M. Feigel'man, "Perturbed kitaev model: Excitation spectrum and long-ranged spin correlations," *Journal of Physics and Chemistry of Solids* **128**, 130–137 (2019), spin-Orbit Coupled Materials.
- [23] S. Mandal, S. Bhattacharjee, K. Sengupta, R. Shankar, and G. Baskaran, "Confinement-deconfinement transition and spin correlations in a generalized kitaev model," *Phys. Rev. B* **84**, 155121 (2011).
- [24] J. c. v. Chaloupka, G. Jackeli, and G. Khaliullin, "Kitaev-heisenberg model on a honeycomb lattice: Possible exotic phases in iridium oxides A₂iro₃," *Phys. Rev. Lett.* **105**, 027204 (2010).
- [25] A. Nanda, K. Dhochak, and S. Bhattacharjee, "Phases and quantum phase transitions in an anisotropic ferromagnetic kitaev-heisenberg- Γ magnet," *Phys. Rev. B* **102**, 235124 (2020).
- [26] A. Nanda, A. Agarwala, and S. Bhattacharjee, "Phases and quantum phase transitions in the anisotropic antiferromagnetic kitaev-heisenberg- Γ magnet," *Phys. Rev. B* **104**, 195115 (2021).
- [27] J. Knolle, S. Bhattacharjee, and R. Moessner, "Dynamics of a quantum spin liquid beyond integrability: The kitaev-heisenberg- Γ model in an augmented parton mean-field theory," *Phys. Rev. B* **97**, 134432 (2018).
- [28] J. G. Rau, E. K.-H. Lee, and H.-Y. Kee, "Generic spin model for the honeycomb iridates beyond the kitaev limit," *Phys. Rev. Lett.* **112**, 077204 (2014).
- [29] S. Banerjee and S.-Z. Lin, "Emergent orbital magnetization in Kitaev quantum magnets," *SciPost Phys.* **14**, 127

- (2023).
- [30] U. Kumar, S. Banerjee, and S.-Z. Lin, “Floquet engineering of kitaev quantum magnets,” *Communications Physics* **5**, 157 (2022).
- [31] S. Banerjee, U. Kumar, and S.-Z. Lin, “Inverse faraday effect in mott insulators,” *Phys. Rev. B* **105**, L180414 (2022).
- [32] H. Takagi, T. Takayama, G. Jackeli, G. Khaliullin, and S. E. Nagler, “Concept and realization of kitaev quantum spin liquids,” *Nature Reviews Physics* **1**, 264–280 (2019).
- [33] Y. Motome, R. Sano, S. Jang, Y. Sugita, and Y. Kato, “Materials design of kitaev spin liquids beyond the jackeli-khaliullin mechanism,” *Journal of Physics: Condensed Matter* **32**, 404001 (2020).
- [34] A. Banerjee, C. A. Bridges, J.-Q. Yan, A. A. Aczel, L. Li, M. B. Stone, G. E. Granroth, M. D. Lumsden, Y. Yiu, J. Knolle, S. Bhattacharjee, D. L. Kovrizhin, R. Moessner, D. A. Tennant, D. G. Mandrus, and S. E. Nagler, “Proximate kitaev quantum spin liquid behaviour in a honeycomb magnet,” *Nature Materials* **15**, 733–740 (2016).
- [35] L. Janssen, E. C. Andrade, and M. Vojta, “Magnetization processes of zigzag states on the honeycomb lattice: Identifying spin models for α - RuCl_3 and Na_2IrO_3 ,” *Phys. Rev. B* **96**, 064430 (2017).
- [36] L. E. Chern, F. L. Buessen, and Y. B. Kim, “Classical magnetic vortex liquid and large thermal hall conductivity in frustrated magnets with bond-dependent interactions,” *npj Quantum Materials* **6**, 33 (2021).
- [37] P. Czajka, T. Gao, M. Hirschberger, P. Lampen-Kelley, A. Banerjee, J. Yan, D. G. Mandrus, S. E. Nagler, and N. P. Ong, “Oscillations of the thermal conductivity in the spin-liquid state of α - RuCl_3 ,” *Nature Physics* **17**, 915–919 (2021).
- [38] N. D. Patel and N. Trivedi, “Magnetic field-induced intermediate quantum spin liquid with a spinon fermi surface,” *Proceedings of the National Academy of Sciences* **116**, 12199–12203 (2019), <https://www.pnas.org/doi/pdf/10.1073/pnas.1821406116>.
- [39] D. Wulferding, Y. Choi, S.-H. Do, C. H. Lee, P. Lemmens, C. Faurgas, Y. Gallais, and K.-Y. Choi, “Magnon bound states versus anyonic majorana excitations in the kitaev honeycomb magnet α - RuCl_3 ,” *Nature Communications* **11**, 1603 (2020).
- [40] C. Berke, S. Trebst, and C. Hickey, “Field stability of majorana spin liquids in antiferromagnetic kitaev models,” *Phys. Rev. B* **101**, 214442 (2020).
- [41] H. Li, T. T. Zhang, A. Said, G. Fabbris, D. G. Mazzone, J. Q. Yan, D. Mandrus, G. B. Halász, S. Okamoto, S. Murakami, M. P. M. Dean, H. N. Lee, and H. Miao, “Giant phonon anomalies in the proximate kitaev quantum spin liquid α - RuCl_3 ,” *Nature Communications* **12**, 3513 (2021).
- [42] C. Balz, L. Janssen, P. Lampen-Kelley, A. Banerjee, Y. H. Liu, J.-Q. Yan, D. G. Mandrus, M. Vojta, and S. E. Nagler, “Field-induced intermediate ordered phase and anisotropic interlayer interactions in α - RuCl_3 ,” *Phys. Rev. B* **103**, 174417 (2021).
- [43] D. Reig-i Plessis, T. A. Johnson, K. Lu, Q. Chen, J. P. C. Ruff, M. H. Upton, T. J. Williams, S. Calder, H. D. Zhou, J. P. Clancy, A. A. Aczel, and G. J. MacDougall, “Structural, electronic, and magnetic properties of nearly ideal $J_{eff} = \frac{1}{2}$ iridium halides,” *Phys. Rev. Mater.* **4**, 124407 (2020).
- [44] S. Biswas, Y. Li, S. M. Winter, J. Knolle, and R. Valentí, “Electronic properties of α - RuCl_3 in proximity to graphene,” *Phys. Rev. Lett.* **123**, 237201 (2019).
- [45] V. Leeb, K. Polyudov, S. Mashhadi, S. Biswas, R. Valentí, M. Burghard, and J. Knolle, “Anomalous quantum oscillations in a heterostructure of graphene on a proximate quantum spin liquid,” *Phys. Rev. Lett.* **126**, 097201 (2021).
- [46] J. Nasu and Y. Motome, “Nonequilibrium majorana dynamics by quenching a magnetic field in kitaev spin liquids,” *Phys. Rev. Res.* **1**, 033007 (2019).
- [47] D. C. Ronquillo, A. Vengal, and N. Trivedi, “Signatures of magnetic-field-driven quantum phase transitions in the entanglement entropy and spin dynamics of the kitaev honeycomb model,” *Phys. Rev. B* **99**, 140413 (2019).
- [48] S. Wang, Z. Qi, B. Xi, W. Wang, S.-L. Yu, and J.-X. Li, “Comprehensive study of the global phase diagram of the $j-k-\Gamma$ model on a triangular lattice,” *Phys. Rev. B* **103**, 054410 (2021).
- [49] J. Nasu, M. Udagawa, and Y. Motome, “Thermal fractionalization of quantum spins in a kitaev model: Temperature-linear specific heat and coherent transport of majorana fermions,” *Phys. Rev. B* **92**, 115122 (2015).
- [50] A. Koga and J. Nasu, “Residual entropy and spin fractionalizations in the mixed-spin kitaev model,” *Phys. Rev. B* **100**, 100404 (2019).
- [51] H. Li, H.-K. Zhang, J. Wang, H.-Q. Wu, Y. Gao, D.-W. Qu, Z.-X. Liu, S.-S. Gong, and W. Li, “Identification of magnetic interactions and high-field quantum spin liquid in α - RuCl_3 ,” *Nature Communications* **12**, 4007 (2021).
- [52] S. Mandal, R. Shankar, and G. Baskaran, “Rvb gauge theory and the topological degeneracy in the honeycomb kitaev model,” *Journal of Physics A: Mathematical and Theoretical* **45**, 335304 (2012).
- [53] M. G. Yamada, “Anderson-kitaev spin liquid,” *npj Quantum Materials* **5**, 82 (2020).
- [54] K. Hwang, A. Go, J. H. Seong, T. Shibauchi, and E.-G. Moon, “Identification of a kitaev quantum spin liquid by magnetic field angle dependence,” *Nature Communications* **13**, 323 (2022).
- [55] S. M. Pervaz and S. Mandal, “Deciphering competing interactions of kitaev-heisenberg- Γ system in clusters,” (2023), [arXiv:2306.14839 \[cond-mat.str-el\]](https://arxiv.org/abs/2306.14839).
- [56] S. Deffner and S. Campbell, “Quantum speed limits: from heisenberg’s uncertainty principle to optimal quantum control,” *Journal of Physics A: Mathematical and Theoretical* **50**, 453001 (2017).
- [57] G. Ness, A. Alberti, and Y. Sagi, “Quantum speed limit for states with a bounded energy spectrum,” *Phys. Rev. Lett.* **129**, 140403 (2022).
- [58] B. Mohan and A. K. Pati, “Quantum speed limits for observables,” *Phys. Rev. A* **106**, 042436 (2022).
- [59] S. Aggarwal, S. Banerjee, A. Ghosh, and B. Mukhopadhyay, “Non-uniform magnetic field as a booster for quantum speed limit: faster quantum information processing,” *New Journal of Physics* **24**, 085001 (2022).
- [60] W. Wang, Z.-Y. Dong, S.-L. Yu, and J.-X. Li, “Theoretical investigation of magnetic dynamics in α - RuCl_3 ,” *Phys. Rev. B* **96**, 115103 (2017).
- [61] A. Maity, Y. Iqbal, and S. Mandal, “Competing orders in a frustrated heisenberg model on the fisher lattice,” *Phys. Rev. B* **102**, 224404 (2020).
- [62] P. d’Ornellas and J. Knolle, “Kitaev-heisenberg model on the star lattice: From chiral majorana fermions to chiral

triplons,” *Phys. Rev. B* **109**, 094421 (2024).

V. APPENDIX

Appendix A: Finite Γ results

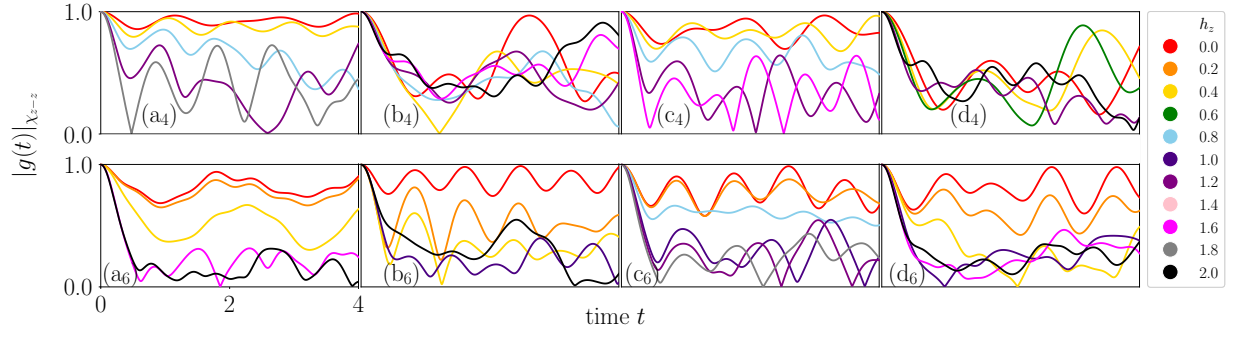


FIG. 10. Gauge Majorana dynamics for $J = 0$ and (a_N) $K = 1.0$, $\Gamma = 0.5$, (b_N) $K = -1.0$, $\Gamma = 0.5$, (c_N) $K = 1.0$, $\Gamma = -0.5$, (d_N) $K = -1.0$, $\Gamma = -0.5$. Different strength of h_z are given in legend box.

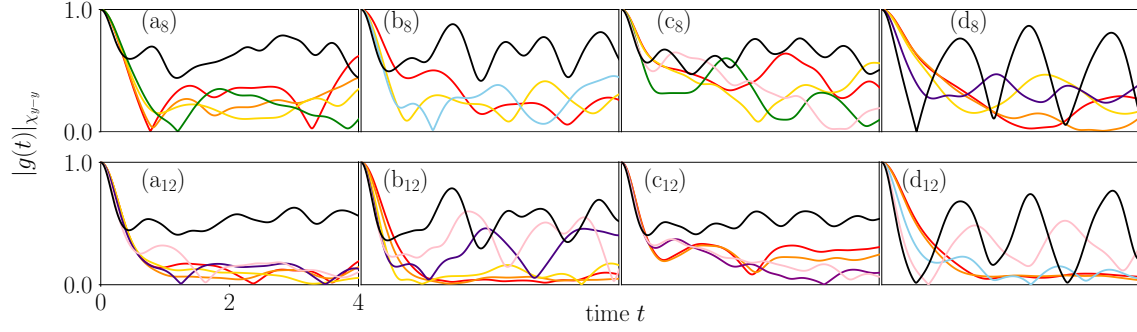


FIG. 11. Gauge Majorana dynamics for $J = 0$ and (a_N) $K = 1.0$, $\Gamma = 0.5$, (b_N) $K = -1.0$, $\Gamma = 0.5$, (c_N) $K = 1.0$, $\Gamma = -0.5$, (d_N) $K = -1.0$, $\Gamma = -0.5$. Different strength of h_z are given in legend box of FIG.10.

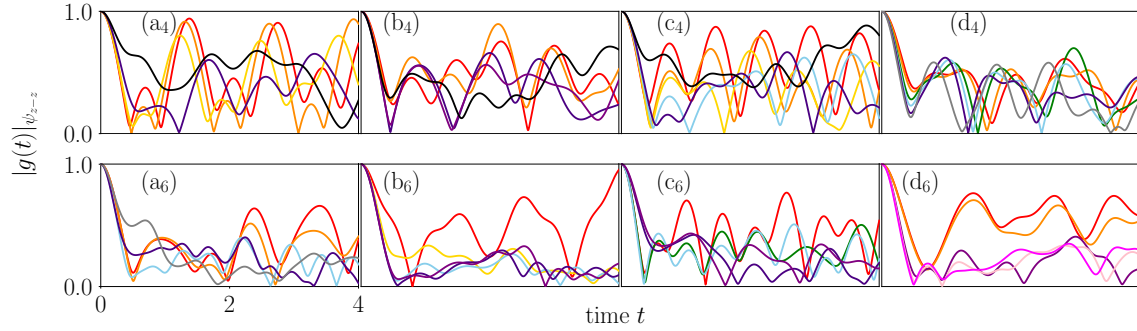


FIG. 12. Matter Majorana dynamics for $J = 0$ and (a_N) $K = 1.0$, $\Gamma = 0.5$, (b_N) $K = -1.0$, $\Gamma = 0.5$, (c_N) $K = 1.0$, $\Gamma = -0.5$, (d_N) $K = -1.0$, $\Gamma = -0.5$. Different strength of h_z are given in legend box of FIG.10.

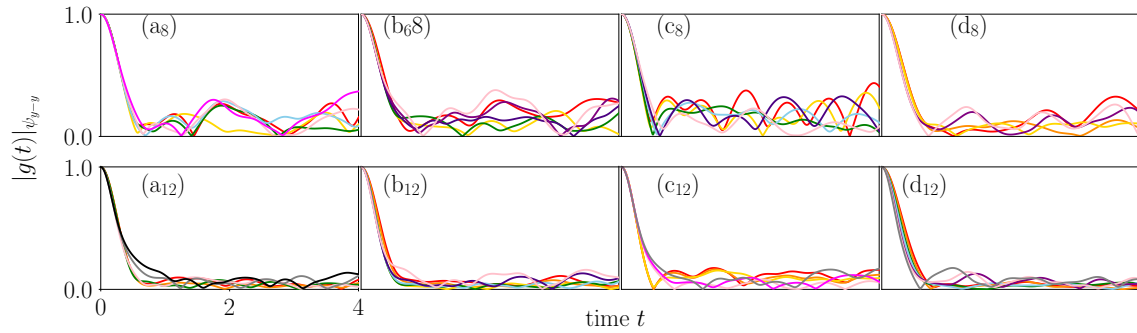


FIG. 13. Matter Majorana dynamics for $J = 0$ and (a_N) $K = 1.0$, $\Gamma = 0.5$, (b_N) $K = -1.0$, $\Gamma = 0.5$, (c_N) $K = 1.0$, $\Gamma = -0.5$, (d_N) $K = -1.0$, $\Gamma = -0.5$. Different strength of h_z are given in legend box of FIG.10.